Available online at www.sciencedirect.com
ScienceDirect
Journal of Solid State Chemistry 180 (2007) 611–618
JOURNAL OF SOLID STATE CHEMISTRY
www.elsevier.com/locate/jssc

A sol–gel route for the development of rare-earth aluminum borate nanopowders and transparent thin films

Lauro J.Q. Maia[a,b,*], Valmor R. Mastelaro[a], Sebastien Pairis[b], Antonio C. Hernandes[a], Alain Ibanez[b]

[a]*Grupo Crescimento de Cristais e Materiais Cerâmicos, Instituto de Física de São Carlos-Universidade de São Paulo, Caixa Postal 369, 13560-970 São Carlos/SP, Brazil*

[b]*Laboratoire de Cristallographie, CNRS, UPR 5031, associé à l'Université Joseph Fourier-Grenoble et à l'INPG, 25 Avenue des Martyrs, BP 166, 38042 Grenoble, France*

Received 29 August 2006; received in revised form 2 November 2006; accepted 13 November 2006
Available online 22 December 2006

Abstract

A new sol–gel route was applied to obtain $Y_{0.9}Er_{0.1}Al_3(BO_3)_4$ crystalline powders and amorphous thin films by using $Al(acac)_3$, $B(OPr^i)_3$, $Y(NO_3)_3 \cdot 6H_2O$, and $Er(NO_3)_3 \cdot 5H_2O$ as starting materials dissolved in propionic acid and ethyl alcohol mixtures. Our study shows that propionic acid acts as good chelant agent for yttrium and erbium ions while ethyl alcohol allows to dissolve $Al(acac)_3$. This process makes the resulting sols very stable to obtain homogeneous gels and transparent amorphous thin films. In addition, the propionic acid prevents the sol precipitation, making easy porous- and crack-free thin film depositions. Chemical reactions involved in the complexation were discussed. As-prepared powders and films are amorphous and present a good thermal stability due to their high glass transition (746 °C) and crystallization temperatures (830 °C). This new sol–gel route showed to be adequate to obtain dense and crack-free thin films free of organic and hydroxyl groups that can be considered as promising materials to be used in integrated optical systems.

Keywords: Sol–gel; Propionic acid; $Y_{0.9}Er_{0.1}Al_3(BO_3)_4$; Nanopowders; Thin films; Thermal analyses; XRD; SEM; FEG

1. Introduction

Growing demand of optical systems and due to their future potentialities, there is stimulating research for devices composing a network system with excellent flexibility and larger information capacities at much faster rates. Among several devices in telecommunication systems, the invention of optical amplifiers [1] can be compared to that of the transistors in electronics in terms of its technological impact. The technology to directly amplify the light signal without the conversion of light/electricity/light has been achieved with rare-earth-doped fibers which realize ideal amplification with high gain and low noise [2]. Optical properties of rare-earth ions incorporated in glass hosts are of great interest in opto-electronic technology [3]. Rare earth trivalent ions in some solid compounds emit light at characteristic wavelengths due to intra-4*f* or internal 4*f*–5*d* transitions. In the case of Er^{3+}, the emission at 1.54 μm corresponds to a dipole forbidden intra 4*f* transition $^4I_{13/2}$ to $^4I_{15/2}$, coinciding with the low-loss window of standard optical telecommunication silica fiber.

Recently, remarkable progress has been achieved in the development of single-mode Er-doped optical fiber amplifiers and lasers [4–6]. Development of Er-doped planar waveguide amplifiers has also been investigated [7,8] to be applied in integrated optical systems, but integrated optical amplifiers should be as small as possible (a few centimeters), so that much higher rare-earth concentrations are required than in Er-doped fiber amplifiers (EDFAs). However, due to the onset of concentration quenching at low doping levels in silica hosts, the relatively low gains/unit length which can be achieved has made such development difficult. Consequently, SiO_2 is an unsuitable host in small, compact amplifiers due to the low erbium solubility.

*Corresponding author. Fax: +55 16 3373 9824.
E-mail address: lauro@if.sc.usp.br (L.J.Q. Maia).

0022-4596/$ - see front matter © 2006 Elsevier Inc. All rights reserved.
doi:10.1016/j.jssc.2006.11.016

Thus, there is a great interest to find other host matrices with high solubility for rare-earth elements, especially erbium, for integrated systems. One potential host candidate is the yttrium aluminum borate ($YAl_3(BO_3)_4$, YAB), where yttrium can be substituted by erbium due to their similar ionic radii (0.096 nm for Er^{3+} and 0.093 nm for Y^{3+}) [9,10]. The YAB composition exhibits good properties for solid-state lasers, high physical and chemical stability, high thermal conductivity, good mechanical strength [11], and a rather high non-linear optical coefficient [12]. Moreover, Er:YAB can be used as a waveguide core ($n = 1.6$–1.7) on SiO_2 substrates ($n = 1.45$). This high refractive index contrast allows a large signal admittance angle and high signal confinement within the core, increasing the pumping and the amplification efficiency [13,14].

In addition, there is a great interest for homogeneous glassy thin films to be used as waveguides because there are no grain boundaries that can cause a high optical loss as in polycrystalline films. The glassy borate system around the YAB composition is very suitable for this purpose because it presents a high glass transition temperature ($T_g \sim 700\,^{\circ}C$). Furthermore, there is interest to obtain a transparent YAB ceramic composition which can be used as laser medium. Recent results presented in the literature confirm that ceramic laser materials became an attractive alternative to single crystal due to their easy manufacture and low cost [15]. In this way, Er-doped YAB matrices are interesting materials for integrated amplifiers and laser medium.

The sol–gel process allows the preparation of bulk materials, thin films as well as powders that can be used to prepare ceramics. The major advantages of this low-temperature chemical route are the large variety of materials that can be doped to modify their properties, the excellent control of the chemical purity, low cost of fabrication and possibility to obtain nanometer powders with a controlled size particle for transparent ceramics manufacture. Since thin sol–gel films can be easily made through dip-coating or spin-coating techniques, this method is considered ideal for the fabrication of active integrated optical devices like optical waveguide lasers and amplifiers [16–19].

In this paper, we present an investigation on the development of a new sol–gel route to obtain homogeneous Er-doped YAB nanometer-sized powders and transparent vitreous thin films free of cracks and porosity with relatively thick monolayers. We describe the chemical reactions of our sol–gel process and the thermal, structural and micro-structural characterizations of the corresponding samples. The results should contribute to establish a new sol–gel route that could be used to prepare other complex materials.

2. Experimental section

2.1. Sol preparation

In this study we have involved aluminum acetylacetonate ($Al(acac)_3$, Aldrich 99%), aluminum nitrate ($Al(NO_3)_3 \cdot 9H_2O$, Prolabo 98%), or aluminum *s*-butoxide ($Al(OBu^s)_3$, Strem 98%) as precursor for aluminum; triethylborate ($B(OEt)_3$, Strem > 98%), tri-*i*-propylborate ($B(OPr^i)_3$, Strem 98%), or tri-*n*-butilborate ($B(OBu^n)_3$, Strem 99%) for boron; yttrium acetate dihydrate ($Y(O_2CCH_3)_3 \cdot 2H_2O$, Aldrich 99.9%), yttrium nitrate hexahydrate ($Y(NO_3)_3 \cdot 6H_2O$, Aldrich 99.9%), or yttrium chloride hexahydrate ($YCl_3 \cdot 6H_2O$, Aldrich 99.9%) for yttrium, and erbium acetate dehydrate ($Er(O_2CCH_3)_3 \cdot 2H_2O$, Aldrich 99.9%), erbium nitrate pentahydrate ($Er(NO_3)_3 \cdot 5H_2O$, Aldrich 99.9%), or erbium chloride ($ErCl_3$, Aldrich 99.9%) for erbium, as source for precursors elements to obtain the $Y_{0.9}Er_{0.1}Al_3(BO_3)_4$.

The precursor's dissolution was first carried out in acetic acid (AcOH, Fischer 99.7%) in airtight silica cells (silica glass flasks) to avoid any solution evaporation. Ethyl alcohol (EtOH, Riedel-de Haen 99.8%), Malic acid (Aldrich 99%), citric acid monohydrate (Aldrich 99.5%), acetylacetone (AcacH, Aldrich 99%) or propionic acid (PropAc, Merck 99%) were also involved to obtain homogeneous initial solutions (sols).

The same procedure was always followed to prepare the sols in a dry glove box (N_2-rich atmosphere). Firstly, the powdered precursors was mixed, secondly the solvent and liquid precursors were added and finally, after complete powder dissolution at 80 °C (2–6 h), pure water was added for the hydrolysis (80 °C—1 h). In all our experiments the relative molar amounts of cation precursors (corresponding to the YAB composition), and water were fixed at: 0.9 Y: 0.1 Er: 3 Al: 4 B: $5H_2O$.

2.2. Powder and thin film preparation and characterization

2.2.1. Homogeneous gels and powders

In order to obtain homogeneous powders, it was necessary to prepare homogeneous gels by controlling the solvent evaporation without any precipitation. Thus, gels and homogeneous powders were prepared by slow solvent evaporation at 80 °C during 14 days, placing the solutions inside silica glass flasks with two holes of 0.7 mm in diameter on the covering. Then, the resulting gels were heated at different temperatures to eliminate the organic compounds and crystallize the YAB composition under O_2-rich atmosphere.

X-ray diffraction (XRD) analyses were performed in transmission geometry in a Siemens D5000 equipped with a nickel filter, Cu $K\alpha 1$ ($\lambda = 1.5406$ Å) radiation and a graphite-diffracted beam monochromator. The weight losses of dried gel powders over a temperature range of 50–980 °C was monitored by Thermogravimetric Analysis (Netzsch, TASC414/3 controller and TG209 cell) under an oxygen atmosphere and heating rate of 2 °C/min. DSC technique (Netzsch, 404 S) was used to evaluate the decomposition reactions of gels and the crystallization of powders (pre-calcined at 400 °C/24 h and 700 °C/24 h) under O_2 atmosphere and heating rate of 2 or 5 °C/min over a temperature range of 50–1000 °C. Powder

morphology was observed using a high-resolution scanning electron microscope (FEG-VP, Supra 35, Zeiss, Germany), operating at 3 kV.

2.2.2. Homogeneous thin films

Before coating deposition, the substrates were cleaned by detergent (Argos, biodegradable anionic surfactant), rinsed with deionized water and immersed in a $HNO_3 + HCl$ (16 $HNO_3 + 28$ $HCl + 56$ H_2O in mol) solution during 5 min. The substrates were rinsed again with deionized water and ethyl alcohol and finally dried through air flow.

The solution stability and quality of thin films was evaluated in terms of solvent evaporation. For this purpose, before thin film deposition, the solutions were placed inside of flasks without covering and heat-treated at 80 °C during 30, 60, 70, 75 and 90 min. The heat-treatment at 80 °C/70 min. promotes an evaporation of solvent around 65% in volume. These partially evaporated solutions were used to elaborate thin films by spin-coating on silica glass substrates. A spin-coater (RC8 SussMicrotech™) with the gyrset technology improves thin film uniformity. Rotation acceleration, rotation speed and spin time were fixed at 500 rpm/s, 2250 rpm, and 5 s, respectively.

The thin film thickness measurements were carried out by a perfilometer (Dektak 32, Veeco) equipment, measuring the step between the thin film and substrate surface. The surface quality of thin films and their chemical compositions were analyzed by a scanning electron microscopy (JEOL 840A) equipped with chemical microanalyzer by energy dispersive X-ray (EDX), operating at 10–35 kV, with tungsten electron emitter and secondary electron detection of samples coated by carbon; and by a high-resolution scanning electron microscope (FEG-VP) (Supra 35, Zeiss, Germany), operating at 3 kV.

Grazing incidence X-ray diffraction (GIXRD) measurements of thin films were performed in a home made diffractometer using a position-sensitive detector (PSD) from Inel. Fe$K\alpha$ ($\lambda = 1.936$ Å) radiation (34 kV/25 mA), a divergence slit of 2 mm, a reception slit equal to 0.6 mm and a plane graphite monochromator were used during the measurements. The incident angle of X-ray beam was fixed at 0.3°, 0.5° or 1°, respectively.

3. Results and discussion

3.1. Preparation of stable sols

Independently of the precursor, combination with AcOH led to the precipitation of amorphous and/or crystalline particles. From the analysis of the XRD patterns of precipitated particles dried at 80 °C and heat-treated at 800 °C, it was generally observed the presence of aluminum and/or yttrium complexes. The aluminum complexes precipitation was then inhibited by the EtOH addition, but yttrium complexes precipitation was not avoided with AcOH. Malic and citric acids were then tested as complexant agents combined with EtOH, but these complexant agents promoted emulsion formation. Following other researchers [20,21], AcacH was used to replace AcOH. The prepared sols using this solvent were sufficiently stable and no precipitations were observed. However, this solvent produced porous and very thin (~20 nm thick) film. So, the use of AcacH was also abandoned.

Finally, propionic acid (PropAc) was able to dissolve the precursors and to maintain all the cations in solution for long time periods (at the present moment, one year) when stored into closed in airtight flasks.

In this work, the solution stability was evaluated using different ratios of PropAc:EtOH (55–85:95–125) in term of precipitation. To prepare the solutions, firstly, a solution containing hydrated rare-earth nitrates and PropAc, in the stoichiometric molar ratio: 0.9 Y:0.1 Er:15 PropAc, was prepared and dissolved at 80 °C/3 h. At room temperature (RT), the first one was added to a second solution containing 3 $Al(acac)_3$:$(95 + x)$ EtOH:$(40 + y)$ PropAc:4 $B(OPr^i)_3$ in mols ($x = 0$–30, and $y = 0$–30), also dissolved at 80 °C/3 h. After mixing, the solution was re-heated at 80 °C/1 h. Then, water amounts from 5 to 15 mol were added at RT and the solution was heated again at 80 °C/1 h. Finally the sol was filtered at RT using 0.2 μm filter porosity. During these heat treatments, the solution was placed into a closed silica glass flask with polypropylene covering.

In summary, to the best of our knowledge, a new route and solvents combination were for the first time used to prepare stable and transparent sols to obtain homogeneous gels of Er:YAB compounds. The success of preparation of stable sols and gels is due to the cation complexation induced by propionate ions in alcoholic solutions, promoting the dissolution and allowing the hydrolysis control of alkoxydes compounds to form an alumino-borate network. In addition, PropAc reduces certainly the reactivity of $B(OPr^i)_3$, thus controlling its hydrolysis. The formation of an alumino-borate network induces a continuous increase of the sol viscosity without phase separation until the preparation of homogeneous gels.

3.2. Powders samples

The $Y_{0.9}Er_{0.1}Al_3(BO_3)_4$ powdered samples were prepared from solutions with propionic acid and ethyl alcohol using a molar ratio of 55:95 as selected for the preparation. The resulting gels were previously dried at 80 °C during 14 days with a slow solvent evaporation inside of silica glass flask with two holes of 0.7 mm in diameter on the covering. These dried gels were used to study the decomposition reactions and crystallizations.

Fig. 1a–b show respectively the TGA and DSC curves of $Y_{0.9}Er_{0.1}Al_3(BO_3)_4$ powder obtained from dried gels. These TGA and DSC measurements were performed under rich-oxygen atmosphere with a flux of 80 mL/min and a 2 °C/min heating-rate.

A small weight loss (6.3%) was observed between 25 and 120 °C due to desorption of the adsorbed moisture and the evaporation of residual solvents. From 120 to 555 °C, another large weight loss (59.4%) was interpreted as due to the decomposition of organic groups in the gel (pyrolysis reactions) (Fig. 1a) [22]. On the other hand, three exothermic peaks around 184, 285 and 357 °C were registered in the DSC curve (Fig. 1b). The sharp and intense peak at 184 °C can be attributed to the elimination of NO_x groups and/or to $H_3C–CH_2–C^+=O$ groups elimination of propionic acid, while the large two other peaks suggest that the decomposition of the organic groups may occur progressively. A very little weight loss (0.7%) was detected between 614 and 700 °C (better visualized in the inset of Fig. 1a), probably due to a residual elimination of –OH or organic groups strongly linked to the metals. Around 820 °C, a small exothermic reaction due to the crystallization process was observed (inset of Fig. 1b), accompanied by another very small weight loss (1.5%) in the range 830–930 °C (inset of Fig. 1a), certainly due to a small boron oxide (B_2O_3) loss. The above results imply that, during the sintering process, the decompostion of the organic groups begins at 120 °C and finishes around 700 °C.

In order to improve the DSC signal corresponding to the crystallization process, the powder was previously heat treated at 400 °C/24 h and at 700 °C/24 h under oxygen-rich atmosphere using a heating rate of 5 °C/min. Fig. 2 shows the DSC curve. XRD pattern (Fig. 3) showed that this powder is amorphous at 800 °C. The corresponding DSC curve displayed in Fig. 2 shows a glassy transition (T_g) at 746 °C while the crystallization process (T_c) began at 830 °C. We can consider that the vitreous powder is very stable since the difference between T_c and T_g is 84 °C. This result is very promising for the preparation of dense glassy thin films without organic groups and boron loss on the

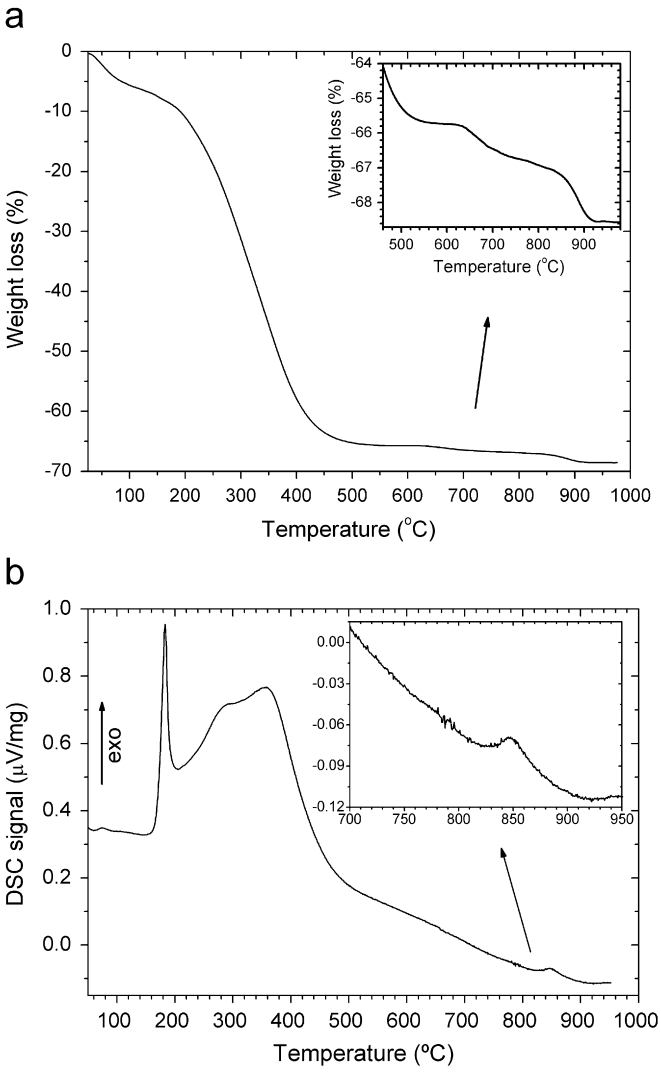

Fig. 1. (a) TG curve of a dried $Y_{0.9}Er_{0.1}Al_3(BO_3)_4$ gel at 80 °C during 14 days, and (b) DSC curve of a dried $Y_{0.9}Er_{0.1}Al_3(BO_3)_4$ gel at 80 °C during 33 h.

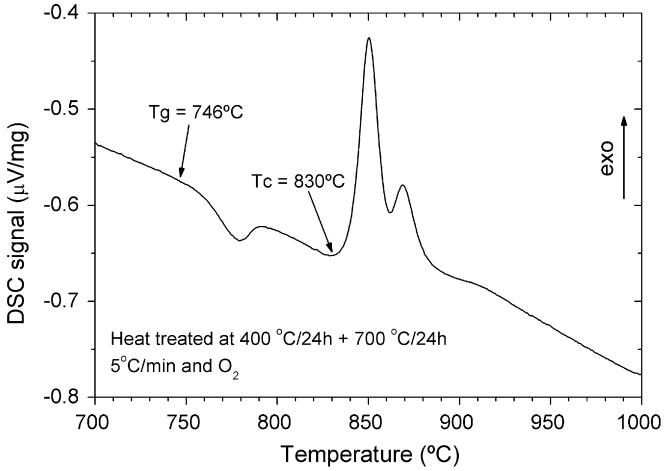

Fig. 2. DSC curves for $Y_{0.9}Er_{0.1}Al_3(BO_3)_4$ powders from dried gels calcined at 400 and 700 °C during 24 h, under O_2 atmosphere.

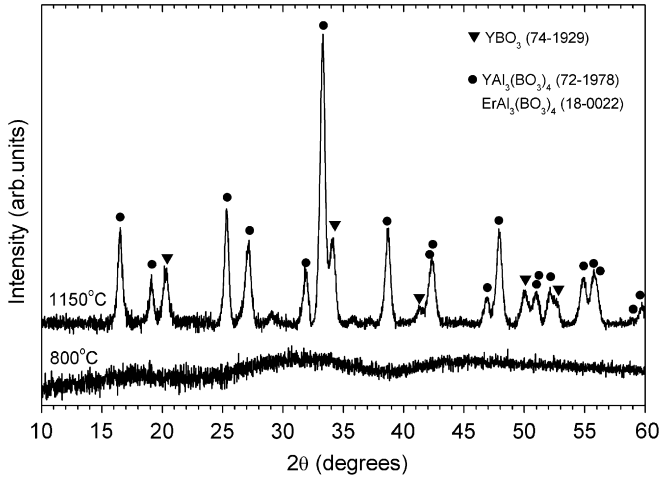

Fig. 3. XRD patterns of $Y_{0.9}Er_{0.1}Al_3(BO_3)_4$ powders heat-treated at 800 °C or 1150 °C under O_2 atmosphere, from powders previously calcined at 400 and 700 °C during 24 h.

746–830 °C temperature range (see next section). The bump on the DSC curve between T_g and T_c (Fig. 2) is due to a significant evolution of boron surroundings (BO_4 to BO_3 transformation) that is associated to strong change of viscosity and specific heat capacity (C_p) of the sample. This effect was already observed by other authors [23–25].

Between 830 and 970 °C, three crystallization peaks are observed (Fig. 2). The first one at 850 °C is mainly due to $Al_4B_2O_9$ and $YAlO_3$ crystallization whereas the second one, centered at 870 °C, is due to $(Er, Y)BO_3$. The peak centered at 915 °C has a very little intensity due to slow kinetic to form the Er:YAB phase. This was determined by a coupled DSC/XRD measurements and is in good accordance with previous works [26,27]. XRD measurements of powders heat-treated at 1000 °C (not presented here), reveal the presence of four phases: $(Y, Er)Al_3(BO_3)_4$, $(Y, Er)BO_3$, $(Y, Er)Al_2(BO_3)_4$, and $YAlO_3$, being $(Y, Er)Al_3(BO_3)_4$ the major phase. According to other works [26,27] on the Y_2O_3–$3Al_2O_3$–$4B_2O_3$ system, the expected $YAl_3(BO_3)_4$ formation by solid-state reactions (whose optimum temperature was about 1150 °C) was proceeded and accompanied by the appearance of YBO_3, and $Al_4B_2O_9$ intermediate phases. The different phases that appeared in our case are related to the synthesis process employed. The chemical process used in this work is based on the mix of the elements at an atomic level producing nanometric particles. The large surface area of these nanoparticles can contain surface inhomogeneities leading to the formation of different crystalline phases. Fig. 3 shows that at 1150 °C, only the $(Y, Er)BO_3$, and $(Y, Er)Al_3(BO_3)_4$ crystalline phases were observed as main phases, in agreement with the work of Beregi et al. [26]. Based in our results, we can suppose that in our powders prepared by a chemical process, different phases are formed and then proceed the crystallization of the $(Y, Er)Al_3(BO_3)_4$ phase. Therefore, to obtain almost pure powders of $(Y, Er)Al_3(BO_3)_4$ phase, it is necessary to apply annealings at 1150 °C. However, we also observed the formation of Er:YBO_3 phase as well as a smaller loss of boron oxide. Thus, a more detailed study of the crystallization process will be necessary. Other experiments are in progress in order to optimize the synthesis of pure $(Y, Er)Al_3(BO_3)_4$ powder with a low initial excess of boron oxide, and working under a well-controlled atmosphere.

Here, O_2-rich atmosphere were used in all heating treatment stages to improve the pyrolysis reactions eliminating organic compounds from the sol–gel process and also promote a well crystallized YAB phase at high temperatures without oxygen vacancies.

Fig. 4 shows nanometer-sized particles observed by scanning electron microscopy (SEM) from a $Y_{0.9}Er_{0.1}Al_3(BO_3)_4$ powder sample heat-treated under oxygen atmosphere at 400 °C/24 h followed by a second treatment at 700 °C/24 h. Finally, the temperature was increased to 1150 °C and then the powder (sample) was immediately cooled to RT at 5 °C/min. Fig. 4a shows grains with size between 60 and 120 nm agglomerated into large particles

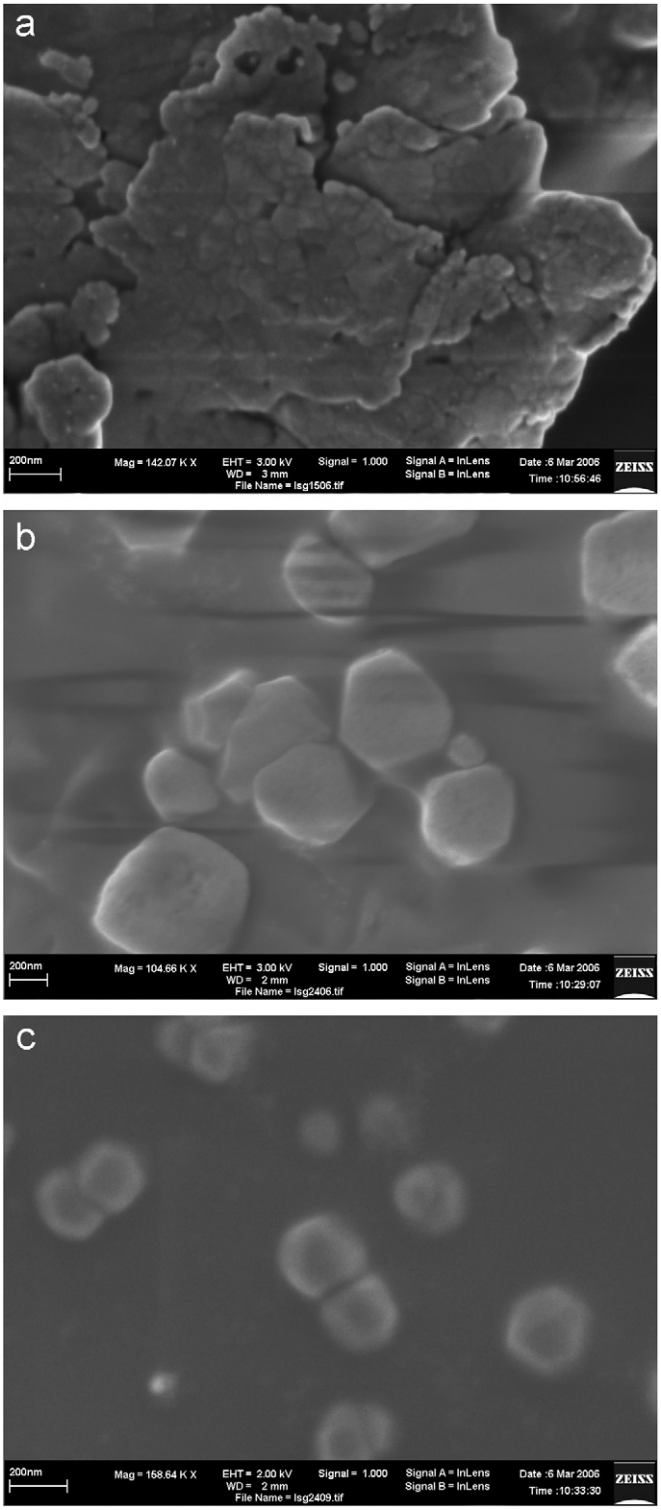

Fig. 4. SEM micrographs of $Y_{0.9}Er_{0.1}Al_3(BO_3)_4$ powders: (a) as calcined at 400 °C and 700 °C during 24 h, and (b)–(c) after heat-treatment at 1150 °C.

with sizes between 300 and 800 nm. This strong agglomeration is due to small grain size and the heat treatment around the T_g which causes the formation of a liquid phase. Fig. 4b shows the microstructure of the powder heat

treated at 1150 °C using a heating-rate of 5 °C/min. We can see defined and faceted nanocrystals exhibiting a size distribution from 190 to 650 nm. The large grain size distribution can be explained by the fact that the powders heat-treated at 700 °C/24 h were vitreous and consequently very fragile. Moreover, the powder was disagglomerated in a mortar before and after heat treatment at 1150 °C. These nanometer-sized powders are very interesting to prepare bulk ceramics. And, also, spherical crystalline nanopowders offer potential for higher definition and brightness in phosphor applications, as suggested by McKittrick et al. [28] and observed by Kang et al. [29].

3.3. Thin films

The EDX technique was used to evaluate the thin films composition heat-treated at 700 °C/2 h and the experimental composition is shown in Table 1. The experimental values are very close to the nominal composition showing good agreement for all elements measured. The boron content was not measured due to low detection efficiency of this element, because this element possesses low-energy X-ray lines (~200 eV).

Fig. 5 shows the thin film monolayer thickness as a function of solvent evaporation time at 80 °C at different molar solvent quantities. Depending on the solvent concentration, and after a heat-treatment of the coating at 450 °C, it was observed that using the as prepared solution (without a later sol drying), we can deposit monolayers with an excellent optical quality and thickness from 12 to 58 nm. Then, by increasing the sol viscosity through a gradual evaporation of the solvent we have linearly raised the film thicknesses (Fig. 5). These results also show that the solutions are stable until a period of evaporation less than 75 min. From solutions dried during 60 min using EtOH and PropAc (95:55), homogeneous monolayers around 130 nm thick were obtained when heat-treated at 450 °C/2 h. Based on the measured thickness, the PropAc:EtOH ratio of 55:95 was selected to prepare gels and films. The obtained thick monolayer (~130 nm) allows the preparation of multilayer coating, around 1 μm thick, supporting at least one guiding mode in 980 nm and in 1530 nm wavelengths.

Table 1
EDX results of $Y_{0.9}Er_{0.1}Al_3(BO_3)_4$ thin film for Y, Er and Al elements

Elements	Composition	
	Experimental	Nominal
Y	0.224 ± 0.005	0.225
Er	0.032 ± 0.004	0.025
Al	0.744 ± 0.005	0.750

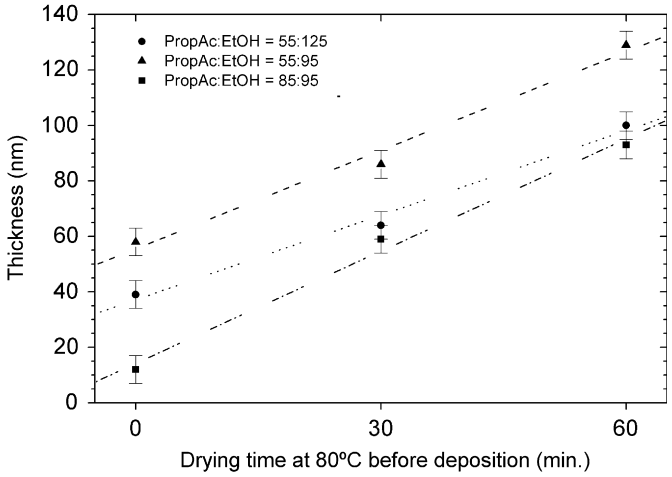

Fig. 5. $Y_{0.9}Er_{0.1}Al_3(BO_3)_4$ thin films thickness from solutions containing different propionic acid and ethyl alcohol proportions as a function of solution drying time at 80 °C before film deposition.

Thin films were also prepared using a molar ratio between PropAc and EtOH of 55:95. Before deposition, the viscosity of the solution was adjusted until 20 mPa s by heating the solution at 80 °C during 70 min. This corresponds to an evaporation of 65% in volume of the solvents. The thin films deposited onto silica glass substrates by spin-coating technique were then heat-treated at 80 °C/30 min, at 400 °C/2 h using a heating-rate of 1 °C/min, and at 700 °C/2 h using a heating-rate of 2 °C/min. Finally, to obtain homogeneous and vitreous thin films without grain boundaries, the samples were submitted to a heat-treatment at 740 °C or 780 °C/2 h just above the T_g temperature with a heating-rate of 1 °C/min.

In this study, to obtain high-quality films, we have simultaneously adjusted two experimental parameters which are directly connected to the formation of cracks: the heating rate and the film thickness. Using heating rates $\geqslant$ 2 °C/min and temperatures between 80 and 400 °C, cracks were observed on the thin film surface (Fig. 6a). Moreover, due to the too rapid gas release during the pyrolysis, we also observed an increase of the film porosity. Using a heating-rate as low as 1 °C/min and a progressive densification near the T_g temperature, we obtained high-quality thin films without any macroscopic defect (Fig. 6b–c). Moreover, the films presented low root-mean-square (RMS) roughness around 0.2 nm, making these films ideal to be used as optical waveguides.

To evaluate the maximum of the layer thickness, without the formation of cracks, was adjusted the solution viscosity by evaporating the solvents. For thin films from solution with EtOH:PropAc = 95:55 previously dried at 80 °C during 70 min. and using a heating rate of 1 °C/min, a limit around 140 nm was found. This limit is not only related to the gas release during the film drying (capillary forces) but also by the difference in the thermal expansion of the film and the silica glass substrate. However, for waveguide application, we should obtain ~800 nm thick films constituted by 6–7 monolayers.

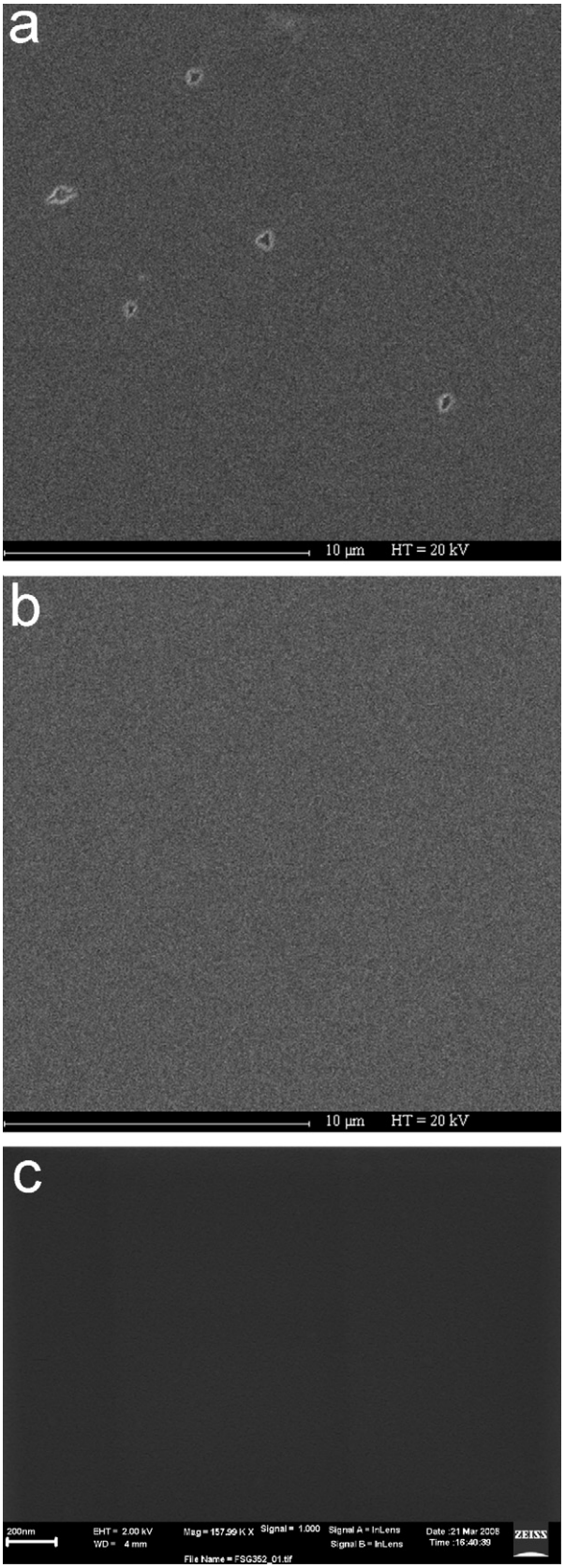

Fig. 6. SEM surface morphology of $Y_{0.9}Er_{0.1}Al_3(BO_3)_4$ thin films heat-treated at 450 °C/2 h: (a) with 2 °C/min heating-rate, and (b) with 1 °C/min heating-rate; and (c) of a film heat-treated at 780 °C/2 h using a 1 °C/min heating-rate.

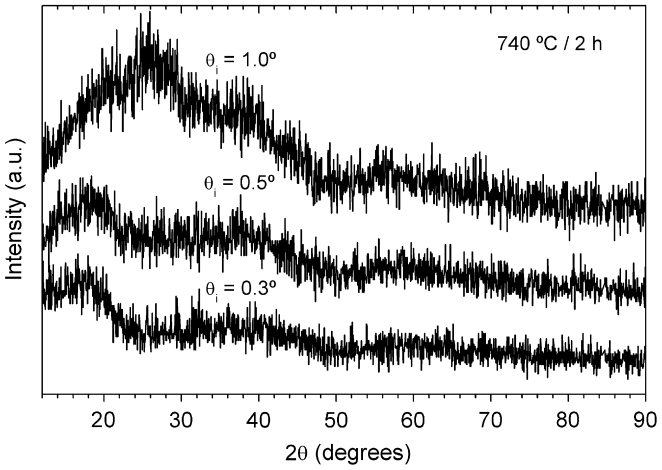

Fig. 7. GIXRD pattern of $Y_{0.9}Er_{0.1}Al_3(BO_3)_4$ thin film heat-treated at 740 °C for 2 h deposited on silica glass as a function of X-ray incidence angle, θ_i, at 0,3°, 0,5° or 1°.

Fig. 7 shows the X-ray pattern of $Y_{0.9}Er_{0.1}Al_3(BO_3)_4$ thin film monolayer deposited on silica glass and heat-treated at 740 °C for 2 h. At this temperature, the film is completely amorphous. When the angle of X-ray incidence increases, we observe a strong X-ray scattering from the silica glass substrate. Similar results were obtained for the films heat treated at 780 °C/2 h.

These results shows that the Er:YAB amorphous thin film is a good candidate to be applied in integrated optics, especially as amplifier waveguides. The heat-treatment above T_g and bellow T_c allows the preparation of homogeneous and uniform thin films which should present a low propagation loss by the surface of thin film.

4. Conclusions

In summary, we have developed a new sol–gel route to prepare $Y_{0.9}Er_{0.1}Al_3(BO_3)_4$ crystalline powders and amorphous thin films which present a good optical quality. We demonstrated that the propionic acid is a better chelant agent especially for Y and Er cations and, when mixed with EtOH, improves the aluminum and yttrium dissolution through their complexation. Using this procedure, we were able to prepare very stable $Y_{0.9}Er_{0.1}Al_3(BO_3)_4$ amorphous powders exhibiting a glass transition temperature at 746 °C and a crystallization temperature around 830 °C. We have also prepared crystalline nanometer sized powders of $Y_{0.9}Er_{0.1}Al_3(BO_3)_4$ composition by annealing the amorphous powder sample at 1150 °C. These nanometer crystallized powders are promising starting materials to prepare bulk ceramics with expected interesting optical properties. Dense and homogeneous vitreous thin films, free of cracks and porous, without the presence of organic groups and boron loss, could be obtained after a heat treatment at temperatures varying from 746 and 830 °C. A multilayer deposition process is in progress in order to produce thick films more adequate to be used as optical waveguides.

Acknowledgments

We acknowledge financial support by the FAPESP (No. 02/13748-9) and CAPES (No. 455/04-1) Brazilian agencies. We thank Dr. Luc Ortega for GIXRD measurements.

References

[1] N. Henmi, Y. Aoki, T. Ogata, T. Saito, S. Nakaya, J. Lightwave Technol. 11 (1993) 1615–1621.
[2] O.N. Krokhin, Laser Phys. 15 (2005) 1303–1305.
[3] S. Mukhopadhyay, K.P. Ramesh, R. Kannan, J. Ramakrishna, Phys. Rev. B 70 (2004) 224202.
[4] O. Polynkin, V. Temyanko, M. Mansuripur, N. Peyghambarian, IEEE Photon. Technol. Lett. 16 (2004) 2024–2026.
[5] C. Cheng, M. Xiao, Opt. Commun. 254 (2005) 215–222.
[6] M.J. Dejneka, B.Z. Hanson, S.G. Crigler, L.A. Zenteno, J.D. Minelly, D.C. Allan, W.J. Miller, D. Kuksenkov, J. Am. Ceram. Soc. 85 (2002) 1100–1106.
[7] D.A.P. Bulla, W.T. Li, C. Charles, R. Boswell, A. Ankiewicz, J.D. Love, J. Lightwave Technol. 23 (2005) 1302–1307.
[8] L. Armelao, S. Gross, G. Obetti, E. Tondello, Surf. Coat. Technol. 190 (2005) 218–222.
[9] R. Martínez Vásquez, R. Osellame, M. Marangoni, R. Ramponi, E. Diéguez, Opt. Mater. 26 (2004) 231–233.
[10] A. Watterich, P. Aleshkevych, M.T. Borowiec, T. Zayarnyuk, H. Szymczak, E. Beregi, L. Kovacs, J. Phys.: Condens. Matter 15 (2003) 3323–3331.
[11] J. Liao, Y. Lin, Y. Chen, Z. Luo, Y. Huang, J. Cryst. Growth 267 (2004) 134–139.
[12] M.H. Bartl, E.C. Fuchs, K. Gatterer, H.P. Fritzer, M. Bettinelli, A. Speghini, J. Solid State Chem. 167 (2002) 386–392.
[13] G. Atanassov, R. Thielsch, D. Popov, Thin Solid Films 223 (1993) 288–292.
[14] P.K. Choudhury, T. Yoshino, Microwave Opt. Tech. Lett. 32 (2002) 359–364.
[15] G. Qin, J. Lu, J.F. Bisson, Y. Feng, K.I. Ueda, H. Yagi, T. Yanagitani, Solid State Commun. 132 (2004) 103–106.
[16] U. Schubert, E. Arpac, W. Glaubitt, A. Helmerich, C. Chau, Chem. Mater. 4 (1992) 291–295.
[17] J. Liu, Y.L. Lam, Y.C. Chan, Y. Zhou, W.X. Que, B.S. Ooi, Appl. Phys. A-Mat. Sci. Process. 69 (1999) 649–651.
[18] C.C. Chang, W.C. Chen, Chem. Mater. 14 (2002) 4242–4248.
[19] M. Zourob, S. Mohr, P.R. Fielden, N.J. Goddard, Lab on a Chip 5 (2005) 772–777.
[20] A.V. Prasadarao, U. Selvaraj, S. Komarneni, A.S. Bhalla, R. Roy, J. Am. Ceram. Soc. 75 (1992) 1529–1533.
[21] N. Özer, J.P. Cronin, Y.J. Yao, A.P. Tomsia, Solar Energy Mat. Solar Cells 59 (1999) 355–366.
[22] V. Jayaraman, T. Gnanasekaran, G. Periaswami, Mater. Lett. 30 (1997) 157–162.
[23] G.D. Chryssikos, E.I. Kamitsos, Y.D. Yiannopoulos, J. Non-Cryst. Solids 196 (1996) 244–248.
[24] J.D. Shelby, Introduction to Glass Science and Technology, The Royal Society of Chemistry, Cambridge, 1997.
[25] L. Cormier, O. Majerus, D.R. Neuville, G. Calas, J. Am. Ceram. Soc. 89 (2006) 13–19.
[26] E. Beregi, A. Watterich, L. Kovács, J. Madarász, Vibrat. Spectr. 22 (2000) 169–173.
[27] J. Madarász, E. Beregi, J. Sztatisz, I. Földvári, G. Pokol, J. Therm. Anal. Calorim. 64 (2001) 1059–1065.
[28] J. McKittrick, B. Hoghooghi, W.B. Dubbleday, K. Kavanagh, K. Kinsman, L. Shea, E. Sluzky, MRS Symp. Proc. 348 (1994) 519–530.
[29] Y.C. Kang, I.W. Lenggoro, S.B. Park, K. Okuyama, J. Solid State Chem. 146 (1999) 168–175.